Improvements of a Molten Carbonate Fuel Cell Power Plant via Exergy Analysis

R. J. Braun
Mechanical Engineering Department,
University of Wisconsin-Madison,
1500 Engineering Drive,
Madison, WI 53706
e-mail: braunr@cae.wisc.edu

R. A. Gaggioli

W. R. Dunbar

Department of Mechanical and
Industrial Engineering,
Marquette University,
Milwaukee, WI 53233

A proposed molten carbonate fuel cell power plant design, intended for commercial production by the end of the 1990s and developed under the auspices of the U.S. Department of Energy, the Gas Research Institute, and Energy Research Corporation, has been analyzed with exergy and pinch analysis. The commercial production units, targeted for dispersed power generation markets, are based on an existing demonstration molten carbonate fuel cell power plant design which was demonstrated from 1996–1997. Exergy analysis of the commercial plant design shows the overall, second-law system efficiency to be 53 percent. The principal inefficiency, 17 percent of the total, lies in the catalytic combustor. Another major inefficiency is the stack loss, 14 percent. Heat transfer accounts for approximately 6 percent of the loss. System reconfigurations, incorporating a steam cycle with reheat (System I) and a gas turbine cycle (System II), both with revised heat exchanger networks, for significant improvement are proposed and evaluated. The second-law system efficiency is raised to 66 percent in System I and to 70 percent for System II.

Introduction

Molten carbonate fuel cells (MCFCs) are experiencing an increasing amount of attention as technological advancements hurdle the problems of cell performance, stack life, and manufacturing costs. The recent advancements coupled with demonstrations of 250-kW and 2-MW MCFC power plants indicate a growth toward a mature technology, one nearly ready for insertion into the dispersed power generation market. The objective of this paper is to use exergy analysis to evaluate the *N*th generation MCFC power plant design and offer alternatives for further improvement in efficiency.

It is acknowledged that the purpose of the demonstration MCFC power plant is to demonstrate carbonate fuel cell technology, particularly power quality, reliability, emissions, and fuel cell (but not plant) efficiency; therefore, it is not an "optimal" design. However, the proposed *N*th generation MCFC power plant design should be analyzed to determine overall plant efficiency and means for improving it. Lobachyov and Richter (1997) investigated the addition of Rankine and Kalina cycles to the *N*th generation MCFC power plant for improved efficiency; however, the addition of a gas turbine cycle was not studied. This paper uses exergy and pinch analysis to propose plant redesigns involving the addition of both steam (System I) and gas turbine (System II) bottoming cycles for substantial gains in electric efficiency and a significant step towards achieving an "optimal" design.

Analysis Methods

The analysis methods used in this study employed basic thermodynamic modeling techniques, which ultimately yield results from the solution of simultaneous governing equations formulated from the system's:

- boundary conditions
- steady-state matter, energy, and exergy balances
- thermodynamic property relations
- performance characteristics of the equipment

The system of equations formulated from the foregoing mathematical model were then solved using Engineering Equation Solver (EES) software for IBM-PCs by F-Chart Software, Middleton, WI.

In this paper, first-law efficiency is defined as the energy ratio of useful products (primarily exported electrical a-c power) to total energy input (primarily fuel input on an HHV basis). Second-law efficiency is defined congruently as the ratio of exergy in useful products (e.g., exported electrical a-c power) to total exergy input (e.g., exergy associated with fuel input to the plant). Evaluation of state point available energies was accomplished following the techniques of Moran (1989) and Rodriguez (1980).

MCFC Operation

Molten carbonate fuel cell stacks consist of repeating fuel cell units, each comprised of an anode, cathode, electrolyte matrix, and a bipolar separator plate between cells (Fig. 1(*a*)). Reactant gases, which typically consist of desulphurized and reformed natural gas and ambient air, flow over the electrode faces (anode and cathode) in channels through the bipolar separator plates generating electrical and thermal energy by the simultaneous electrochemical oxidation of fuel and reduction of oxygen.

The oxidant entering the cathode is an air-CO_2 mixture. Oxygen, carbon dioxide, and electrons react at the cathode to form carbonate ions CO_3^{2-} (Fig. 1(*b*)). These ions transport charge through the molten carbonate electrolyte to the fuel electrode (anode) where they react primarily with hydrogen. The natural gas entering the fuel cell is reformed internally producing hydrogen and carbon monoxide from methane and steam. Hydrogen entering the anode channels is adsorbed into the anode and oxidized by reacting with the carbonate ions to form water and carbon dioxide, and releasing electrons at an electrochemical potential greater than that in the cathode (Williams, 1966).

Water produced from the oxidation of hydrogen reacts with carbon monoxide within the cell to produce additional hydrogen for electrochemical use. This "water-gas shift reaction" ($CO + H_2O = H_2 + CO_2$) is possible because the reaction rapidly reaches equilibrium at the high operating temperature of the fuel cell (Kinoshita et al., 1988). Since carbon dioxide is consumed at the cathode and produced at the anode, anode exhaust gas is typically sent to a combustor for "afterburn," then looped back to the cathode where CO_2 is required.

Contributed by the Advanced Energy Systems Division and presented at the International Mechanical Engineering Congress and Exposition, the Winter Annual Meeting of The American Society of Mechanical Engineers, Atlanta, Georgia, November 17–22, 1996. Manuscript received by the AES Division, March 14, 1997; revised manuscript received July 18, 1999. Associate Technical Editor: W. J. Wepfer.

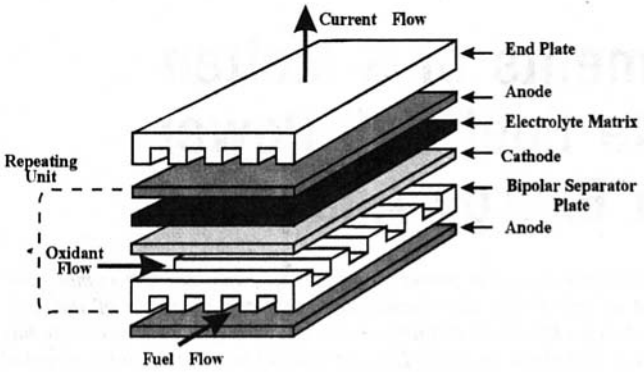

Fig. 1(*a*) Fuel cell stack components

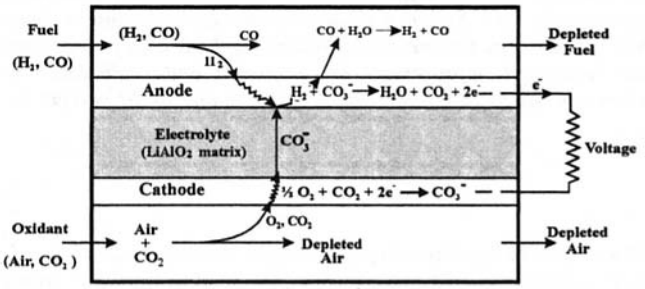

Fig. 1(*b*) Chemical reacting system within an MCFC

2-MW *N*th Generation MCFC Plant Operation

Figure 2 depicts a schematic flow diagram of a 2-MW demonstration power plant. Pipeline natural gas enters the plant at station 1, is preheated to 371°C (700°F) and fed to the fuel gas treatment system where sulfur, a poison to molten carbonate fuel cells, must be reduced to a concentration of 0.1 ppm (EPRI, 1993).

Prior to entering the hydrodesulphurizer (HDS) unit, a small quantity of pure hydrogen gas from the reformer is added to the fuel stream for the purpose of hydrogenating the sulfur compounds. Inside the HDS unit, the natural gas passes over a catalyst converting the sulfur compounds to H_2S for adsorption onto ZnO pellets. Pure hydrogen gas is provided via a steam-methane reformer which is supplied by a mixture of pipeline natural gas and superheated steam from station 17. The reformer is used strictly for the purpose of desulphurization. The desulphurized gas exits the fuel treatment system at station 3 and is mixed with superheated steam (station 16) at a steam-to-carbon ratio of 1.5:1 (EPRI, 1993). This low-pressure steam is added to the clean natural gas to prevent carbon deposition in the fuel cells and fuel gas heaters. Before admittance to the anode compartment of the MCFC, the fuel-steam mixture is superheated to a temperature of 566°C (1050°F) in the fuel superheater (station 5).

The high operating temperature of the molten carbonate fuel cell enables internal reforming to take place with the help of a reforming catalyst, often Ni pellets (Shinoki et al., 1992). Thus, conditions are thermodynamically favorable for the steam-reforming reaction $CH_4 + H_2O \rightarrow CO + 3H_2$. Within the internally reforming fuel cells, the exothermic oxidation of fuel, and the heat

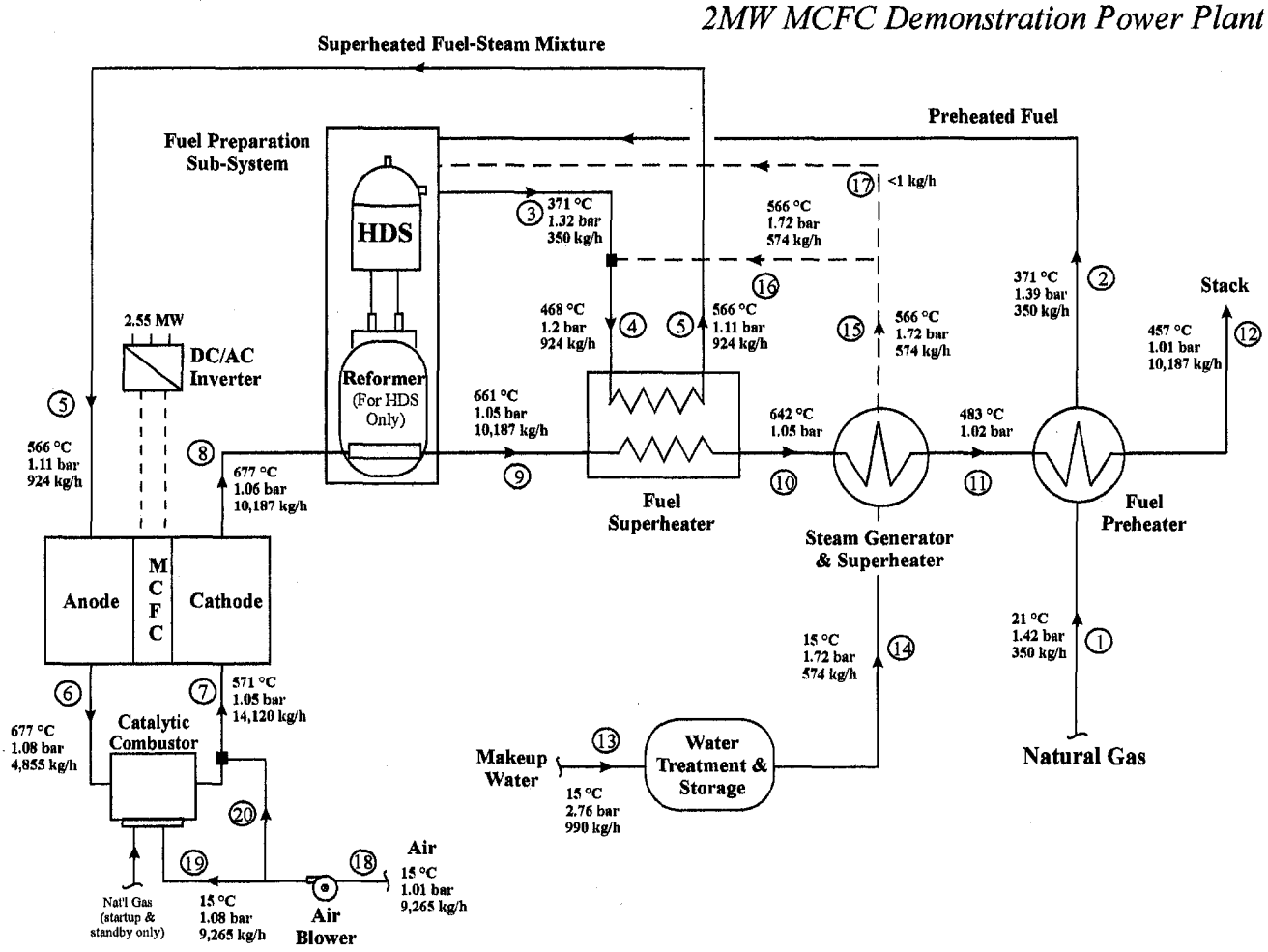

Fig. 2 Process flow diagram

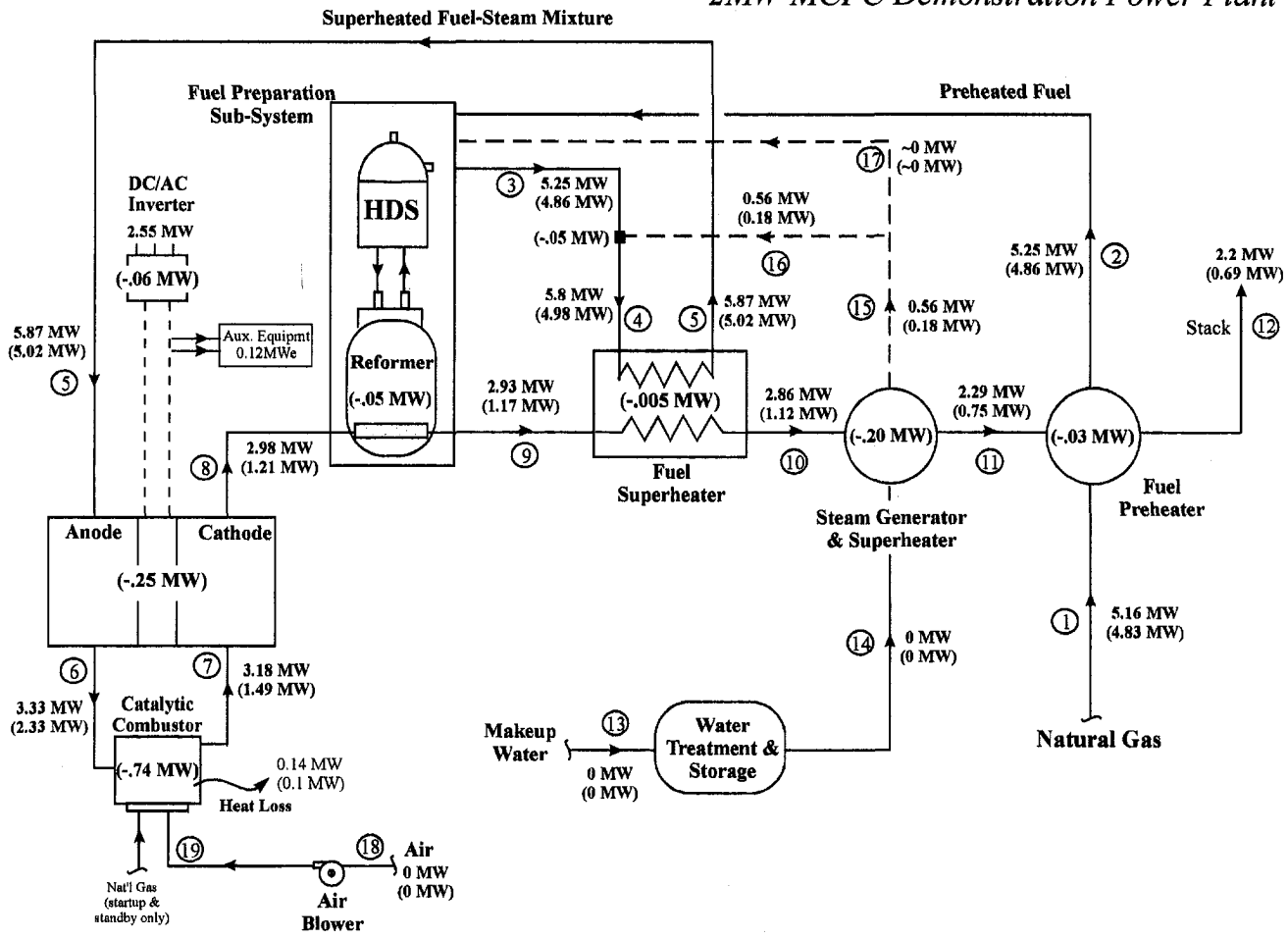

Fig. 3 Energy and exergy flow diagram

generated from cell resistances provides the necessary heat for the endothermic methane reforming reaction, allowing methane to be reformed to hydrogen and carbon monoxide, which is further reacted via the water-gas shift reaction to generate additional hydrogen.

The fuel cell in this design operates at an average cell voltage of 760 mV at 215 mA/cm^2 and a fuel utilization[1] of 78.5 percent consuming most of the hydrogen and generating carbon dioxide (EPRI, 1993). The chemical energy of the fuel is converted to d-c power and heat. At full load, about 2.72 MW of electricity (d-c) is generated. The d-c power generated is inverted to a-c at an efficiency of 97 percent. The depleted fuel exits the anode (station 6) near 677°C (1250°F) and is admitted to the main burner.

Ambient air is supplied to the power plant at station 18, and fed from the air blower to the main burner where it mixes with the hot spent fuel gas. The main burner is outfitted with catalyst to combust low-BTU gas. The combusted gas exits the catalytic combustor at station 7 near 571°C (1060°F) and is used as the oxidant in the cathode of the fuel cell. In addition to burning off the remaining fuel content of stream 6, the combustor provides the extra CO_2 for the cathodic reactions, thus maintaining a positive partial pressure along the cathode channels.

The oxidant stream exhausts from the cathode at 677°C (1250°F) and is fed to the heat recovery units, where the hot gas provides heat for external reforming, superheating the fuel-steam mixture, generating steam, and preheating fuel. The effluent gas is finally vented through the stack to the atmosphere at high temperature, about 457°C (855°F, station 12).

The water side of the plant is small; 990 kg/h (2183 lb/h) of makeup water enters the plant at station 13 and is treated via a reverse osmosis (RO) unit and deaerator before admittance to the boiler/superheat unit. Due to the rejection rates in the RO unit, nearly 50 percent of the water taken in is allowed to drain to the sewer. However, the steam required to achieve the proper steam-to-carbon ratio in the fuel necessitates at least 574 kg/h (1266 lb/h) of water enter the boiler/superheat unit.

Thermodynamic Evaluation

First-Law Analysis. Figure 3 depicts an energy and exergy flow diagram of the plant. Exergy flows are shown parenthetically and destructions within each piece of hardware are depicted as negative quantities. At full load operation, the energy input of the fuel is 5.16 MW (HHV), and 2.67 MW of electricity (a-c) are produced within the fuel cell. The corresponding fuel cell electric efficiency, defined as the ratio of electrical a-c power output to the energy input with the fuel, is 52 percent. The *system* first-law efficiency is 49.5 percent, which corresponds to a heat rate of 6895 BTU/kWh. The auxiliary power requirements (mainly due to pump and blower operation) total nearly 120 kWe. The net power output of the plant is 2.55 MWe at beginning of life (BOL).

Of the 50.5 percent of energy wasted during operation, 42.5 percent are expelled with the stack gas, 4 percent are due to heat losses, 2 percent is from parasite power requirements, and 1 percent is lost in d-c to a-c inversion. From a first-law viewpoint,

[1] Fuel utilization is defined as moles of H_2 consumed over the moles of H_2 and CO fed to the cell (see Kinoshita et al., 1988).

the apparent energy inefficiency is mostly in the form of the high-temperature stack gas. Since the power plant design is targeted for dispersed power generation markets, use of the stack gas for cogeneration or other purposes may still occur on site.

On a first-law basis, improvement of plant performance seems to lie solely in making use of the high-temperature stack gas. There is a sufficient amount of waste heat rejected that could be better served to generate high-pressure steam which would enable the use of a conventional bottoming cycle to increase plant power output, and hence efficiency. The first-law analysis, however, does not properly indicate a target for cycle power output, nor other significant areas for improvements. Hence, a second-law analysis has been employed to reveal and quantify the inefficiencies in the plant.

Second-Law Analysis. An exergy flow diagram is provided in Fig. 3. At full load operation the exergy input with the fuel is 4.83 MW, (about 94 percent of the 5.16 MW HHV).[2] Of the 4.83-MW input, 2.55 MW is electrochemically converted to electricity for export and the balance (2.28 MW) is either destroyed within or lost from the equipment.

The second-law *system* efficiency is 53 percent. This reasonably high exergetic efficiency is attributed solely to the high electric efficiencies attainable with molten carbonate fuel cells. The exergy content in the high-temperature stack gas amounts to 0.69 MW, or over 14 percent of the exergy input with the fuel. Use of the high-temperature stack gas for some conventional bottoming cycle could enhance efficiency by some 10 percent.

Interestingly, exergy balances show that the largest destruction lies in the catalytic combustor, 0.84 MW (including irreversible heat transfer to the surroundings), approximately 17 percent of plant exergy input and nearly 37 percent of the total exergy destructions in the plant. Additionally, 0.25 MW is destroyed or lost in the fuel cell and 0.20 MW in the steam generator and superheater. Exergy destruction due to mixing of the superheated steam and desulphurized fuel stream is only 0.05 MW (or 1 percent of the plant exergy input). The exergy destructions/losses in the fuel preparation sub-system, fuel preheater, and fuel superheater total less than 2 percent of the exergy input to the plant.

Evaluating the exergy destructions in the catalytic combustor reveal that of the 0.84 MW of available energy destroyed/lost in the unit, 0.43 MW are due to mixing, 0.31 MW to the irreversible combustion process, and 0.1 MW through heat transfer to the surroundings. Further study of the losses due to *mixing* indicates that approximately 0.21 MW are annihilated due to *thermal equilibration* and 0.22 MW to *diffusion* processes. In addition to the exergy destruction associated with chemical kinetics, a large part of the 0.31 MW destroyed by combustion is attributable to feeding low-temperature gases to the combustor (Dunbar and Lior, 1991).

A temperature versus amount of heat transfer ($T - Q$) diagram for the cathode exhaust heat exchangers is shown in Fig. 4. The minimum pinch temperature for the network is 76°C (137°F), occurring in the steam superheater. However, in the boiler, where the largest amount of heat transfer takes place, the pinch temperature is 368°C (660°F). The large temperature differences in the heat recovery section provide large driving forces for heat exchange, and hence, low heat transfer area requirements. While design philosophy of this sort may be dictated by cost concerns and plant footprint, penalties are paid in the destructions of available energy associated with heat transfer through large temperature differences.

Assuming that fuel cell performance is state-of-the-art, the targeted inefficiencies for improvement of system performance should be those in the catalytic combustor, boiler-superheater, and that expelled in the stack gas.

[2] Due to the lower valuation of fuel exergy (versus fuel heating value), the resultant exergetic electric efficiency will be higher than a first-law definition.

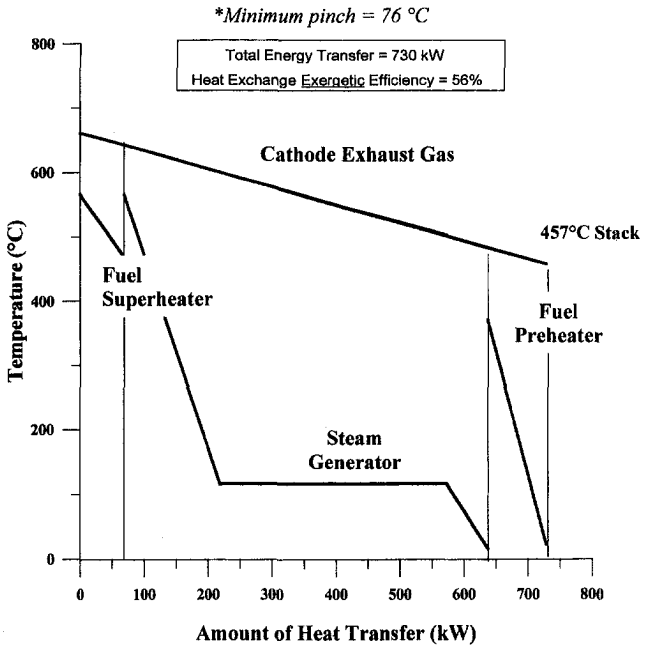

Fig. 4 $T - Q$ diagram of heat recovery exchangers in 2-MW demonstration MCFC power plant

System Redesigns

Goals and Targets for System Redesign. The primary goals for improving the MCFC system design were to reduce the exergy destructions or losses of (*i*) the catalytic combustor, (*ii*) the boiler/superheater unit, and (*iii*) the high-temperature stack gas, in order to increase the power output from the plant. Based on the discussion of the previous section, reducing the exergy destructions in the catalytic combustor by 0.4 MW is a reasonable target. This quantity is comprised of recapturing about 0.2 MW of available energy from thermal mixing and 0.2 MW from combustion. Preheat of combustion air was chosen as a method for achieving this goal. Curtailing annihilations in the steam generator by 50 percent appear feasible by using a lower temperature heat source of appropriate heat capacity for the boiling process. Use of the high-temperature stack gas for preheat of the combustion air would contribute to reducing exergy destructions in the catalytic combustor, and simultaneously address goal (*iii*). By achieving the foregoing targets, recapturing a total of 1 MW of available energy would be feasible—a large fraction of which could then be used to produce more electric power.

Two system redesigns are presented: System I incorporates a steam cycle with reheat, and System II uses an open gas turbine cycle with air as the working fluid.

System I Operation. A process flow diagram of System I is shown in Fig. 5. The design concept employed a high and low-pressure turbine stage with one stage of reheat, operating at 172 bars/593°C/593°C, and no feedwater heaters. The steam power cycle outputs 650 kWe of electricity, boosting net plant electrical output to approximately 3.2 MW.

The design makes use of the high-temperature cathode exhaust gas to preheat air for catalytic combustion and use the subsequent heat gain to drive the steam power cycle. The fuel cell process requirements, that is, inlet and outlet conditions to the fuel cell, were maintained at the design points established in the demonstration plant described in Fig. 2. Additionally, it should be noted that the reformer depicted downstream of the fuel cell (station 9-10) has been broken out of the fuel preparation sub-system of the original plant depicted in Fig. 2, but its purpose of generating hydrogen for the desulfurization process remains unchanged.

Ambient air at 15°C (60°F) enters the plant at station 23 and is

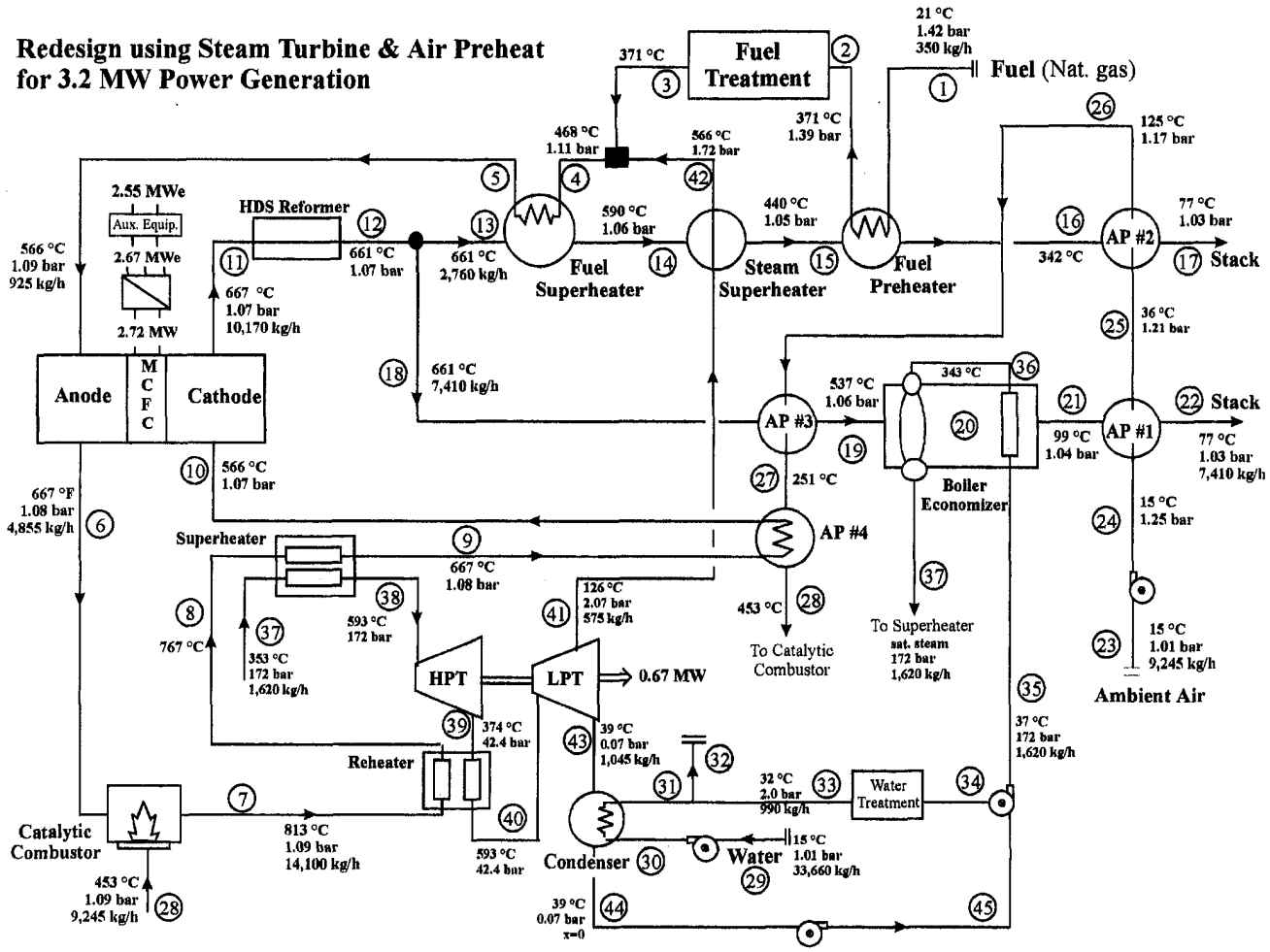

Fig. 5 System I process flow diagram

heated to 453°C (850°F) in four air preheaters. At station 28, the high-temperature air is admitted into the catalytic combustor. Following combustion, exhaust gases exit at station 7 near 815°C (1500°F). (Note: for system redesigns, it is assumed that the high-temperature catalyst in the catalytic combustor, or another catalyst with the same function, can withstand and operate effectively under the new design parameters.)

Subcooled liquid, from the condenser, enters the boiler/economizer at station 35 at a pressure of 172 bars (2500 psia). After flowing through the steam superheater, 593°C (1100°F) steam is delivered to the high-pressure turbine (station 38). The steam expands to 42 bars (615 psia) prior to the reheat stage. Steam necessary for fuel reforming is extracted from the low-pressure turbine at 2 bars (30 psia); the remainder of the steam flow expands to the condenser pressure of 0.07 bars (1 psia).

The cathode exhaust gas is split at station 12 to attain better matching of stream heat capacities in the heat recovery network. Cathode exhaust gases exit the plant at stations 17 and 22, near 77°C (170°F), decreased from 457°C in the original plant design.

First-Law Analysis. Figure 6 displays an energy and exergy flow diagram of System I. The net plant power output is 3.2 MWe, yielding a first-law efficiency of 62 percent and an exergetic efficiency of 66 percent, compared to the demonstration unit design of 49.5 and 52 percent, respectively.

As before, the fuel energy input to the plant remains constant at 5.16 MW. However, in the improved design, an additional 650 kWe of electricity is generated by the high and low-pressure turbines. Also, the effluent losses have been reduced from 2.2 to 0.95 MW, a 57-percent decrease. The resultant net plant heat rate is 5500 Btu/kWh.

Utilizing pinch techniques developed by Linnhoff et al. (cf. 1978 and 1982), a *composite* $T - Q$ diagram of all heat exchanger network streams was constructed and is shown in Fig. 7. A 7°C pinch occurs in the condenser, where 650 kWe of cold utility in the form of lake or river water is required. The largest temperature differences occur primarily in the steam superheater and reheater, where steam turbine inlet temperatures are limited by metallurgical constraints to maximum temperatures of about 600°C (1100°F) (El-Wakil, 1984; Moran and Shapiro, 1992). In comparison with Fig. 4, it is apparent that the match between hot and cold streams is improved, as demonstrated by the decrease in pinch points along the range of heat transfer.

Second-Law Analysis. Exergy flows for the improved design case are also shown in Fig. 6. Of immediate note is the 0.46-MW of exergy destruction and loss in the catalytic combustor; a decrease of 45 percent from the prototype design. The available energy "savings" are credited to reduced exergy destructions associated with thermal mixing of the anode exhaust and combustion air streams, as well as achieving the combustion at higher temperatures by preheating combustion air.

Further decreases in exergy destructions were realized in the boiler and superheater units. The improved use of available energy in these units amounts to a 52-percent savings; reducing exergy destructions from 0.21 to 0.1 MW. The exergy content expelled to the environment with the cathode exhaust gas has been reduced from 0.69 to 0.15 MW, a 78-percent improvement.

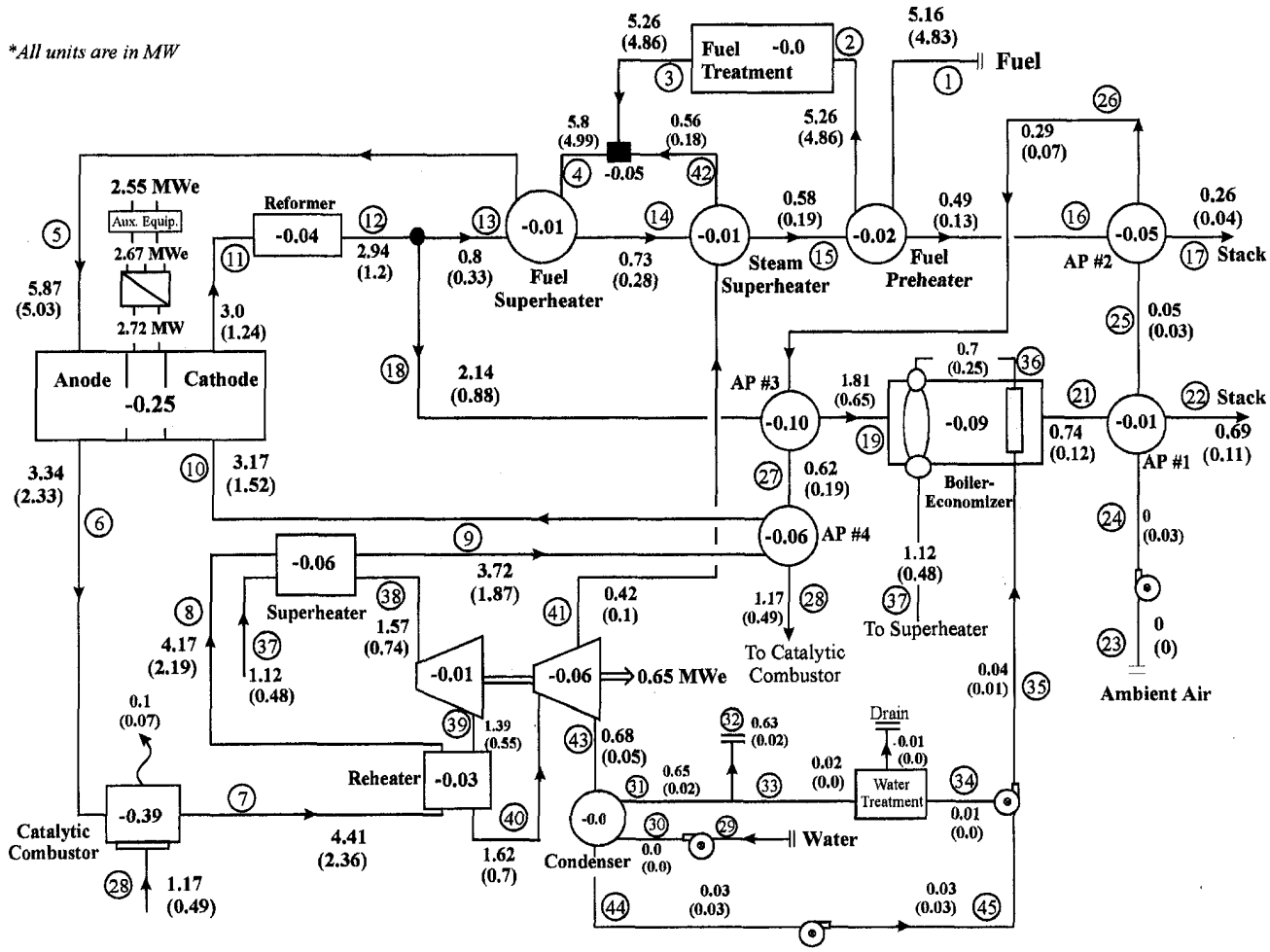

Fig. 6 System I energy and exergy flow diagram

Thus, for System I, a total of 1.34 MW of exergy was recouped and converted to 0.65 MW of electricity for export. This corresponds to a sub-system (i.e., steam turbines and ancillary equipment not found in the *demonstration* plant design) exergetic efficiency of 48.5 percent. The largest portion of exergy destructions, accounting for 68 percent off the total, lie in the heat exchanger network. This is exhibited graphically by a $(1 - To/T)$ versus Q diagram in Fig. 8. The area between the curves is representative of the exergy consumption due to heat transfer. Due to the relatively low second-law efficiency of the heat exchange network (65 percent), another system redesign was made to improve the system efficiency further via incorporating a gas turbine cycle (in the place of a steam one) into the plant.

System II Operation. Figure 9 depicts a process flow diagram for System II. As before, fuel cell operating parameters were maintained at the design points established in the demonstration plant described in Fig. 2. Since the use of gas turbines readily permits inlet turbine temperatures of 1300°C (2400°F), combustion air was preheated as high as the configuration allowed (620°C/1150°F). Following combustion, exhaust gases exit at station 7 near 905°C (1665°F). The heat gain by the cathode inlet gas is used for heat transfer to an open gas turbine cycle. Exhaust air from the turbine is used for regeneration, heat recovery boiling, and air preheat.

The compressor operates at a pressure ratio of 4.5:1, with an 85-percent efficiency. After regeneration and heat addition, air at 880°C (1615°F) and 4.5 atm enters a 90-percent efficient turbine to produce 822 kW of shaft work. A 98-percent efficient generator converts turbine shaft work to 805 kWe of electricity.

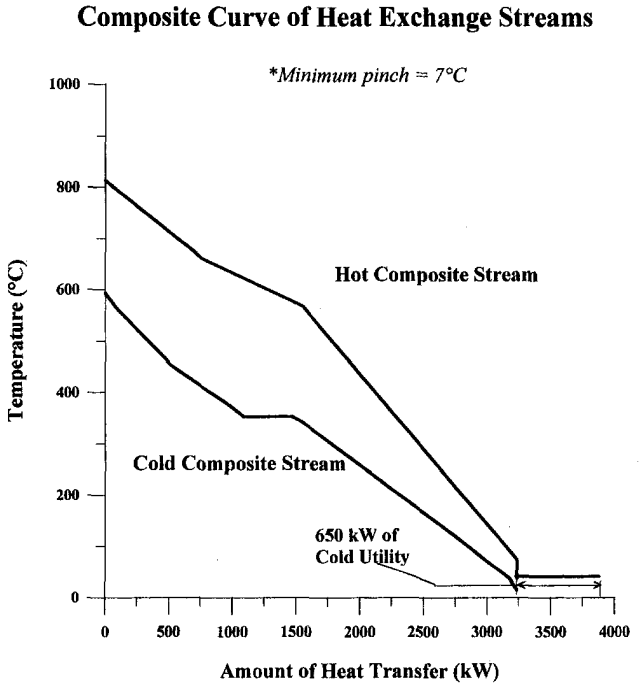

Fig. 7 $T - Q$ diagram, System I: steam turbine configuration

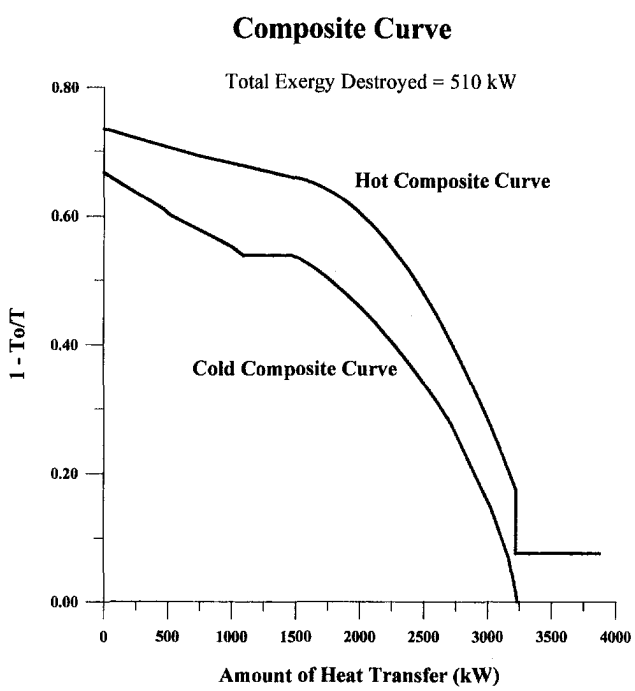

Fig. 8 1 − *To/T* diagram, System I: steam turbine configuration

First-Law Analysis. Figure 10 illustrates an energy and exergy flow diagram for System II. Exergy destructions are shown as negative quantities within each piece of equipment. The net plant power output is 3.35 MWe, yielding a first-law efficiency of 65 percent and a net plant heat rate of 5250 Btu/kWh. The exergetic efficiency is 69.5 percent, a 17-percent improvement over the demonstration plant design and a 4-percent increase over System I.

Figure 11 depicts a composite $T - Q$ diagram of the heat exchange streams in System II. The hot and cold streams closely match each other. A minimum pinch of 15°C (25°F) occurs in several places throughout the plant. Comparison of Fig. 11 with Figs. 4 and 7 clearly illustrates the superior heat exchange network design ("superior" in terms of maintaining small pinches and, therefore, lower exergy destructions).

Second-Law Analysis. Exergy flows for the System II design case are also shown in Fig. 10. Destructions in the catalytic combustor were reduced to 0.34 MW, a decrease of over 50 percent from the demonstration plant design (13 percent over System I). While stack effluent exergy flow increased slightly, lower destructions in the boiler and superheater units were achieved. Overall, the addition of gas turbine and ancillary equipment in System II consumes only 0.19 MW of exergy, while augmenting plant power generation by 805 kWe.

The thrifty use of exergy "transfers" in the heat exchange equipment is illustrated graphically by a $(1 - To/T)$ versus Q diagram in Fig. 12. The exergy consumption totals only 0.23 MW for 3.27 MW of exergy transfer. This corresponds to an exergetic efficiency of 93 percent for the heat exchangers. By comparison, the 2-MW MCFC demonstration plant destroys 0.21 MW of

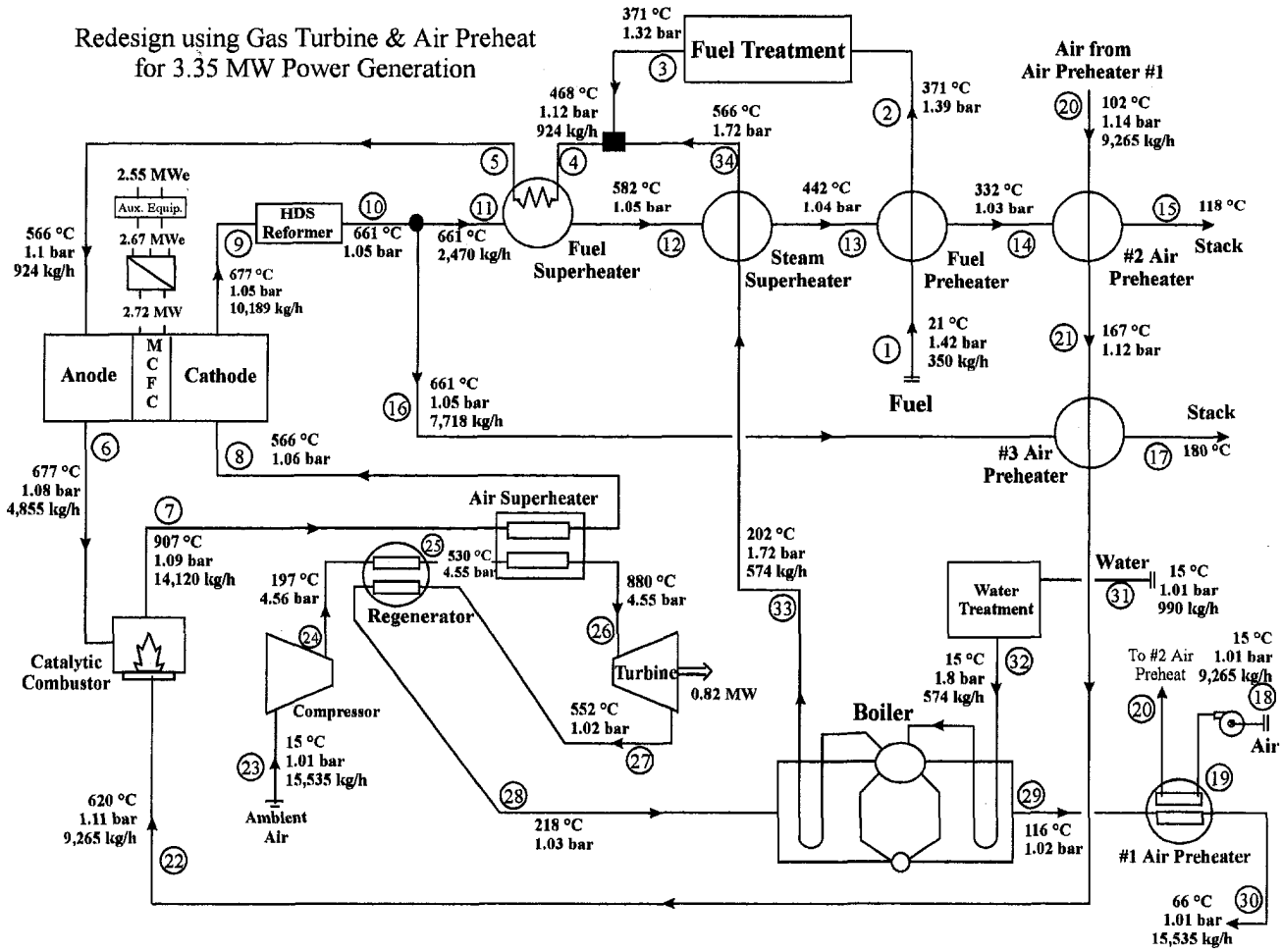

Fig. 9 System II process flow diagram

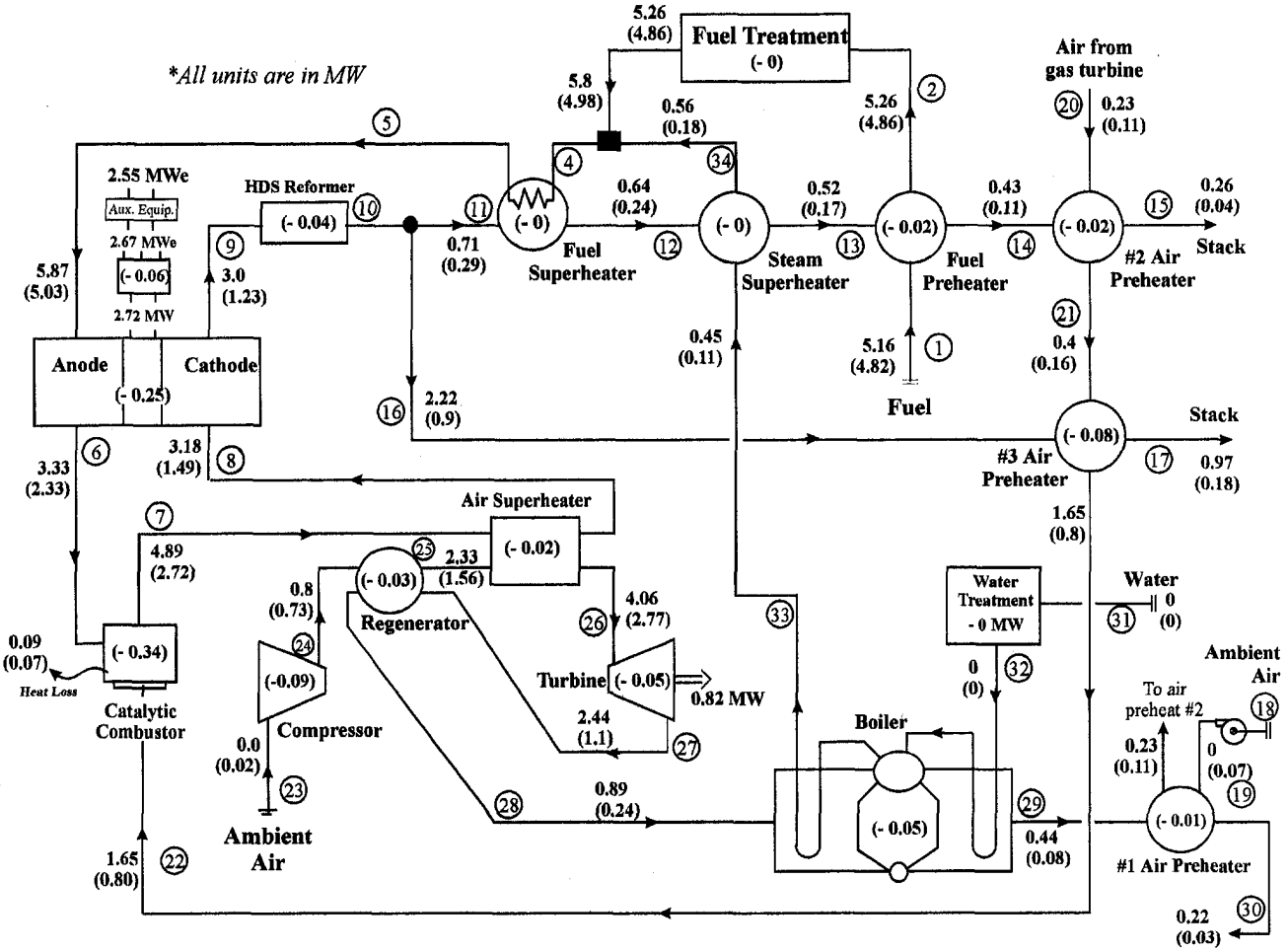

Fig. 10 System II energy and exergy flow diagram

exergy, while transferring only 0.48 MW for a low-exergetic efficiency of 56 percent. Transformation of Fig. 4 from a $T - Q$ diagram to a $(1 - To/T) - Q$ diagram proves unnecessary as the overall shape and spacing of the curves remain nearly unchanged. Thus, simply juxtaposing Fig. 12 with Figs. 4 and 8 gives a good graphical comparison of exergetic efficiencies of all three heat exchanger network designs.

Conclusions

The use of exergy and pinch analysis proved exceptionally useful in pinpointing, quantifying, and illustrating the inefficiencies of the 2-MW MCFC demonstration plant and in guiding the design efforts of Systems I and II. Ultimately, the reconfigurations of Systems I and II posted 14 and 18 percent improvements, respectively, in second-law efficiency by preheating combustion air, lowering pinch temperatures in the boiler and heat exchange equipment, mitigating the exergy losses associated with stack gas effluent, and incorporating a steam or gas turbine cycle to increase power output. The design of System II proved to be more efficient than System I primarily due to the higher exergetic efficiency of the heat exchanger network. Further augmentation of System I performance could almost certainly be accomplished by additional "tweaking" of the heat exchanger network design. However, due to the temperature constraints of steam turbine blading, System I efficiency performance will not attain the level set by System II, with the current goal of producing only power.

Areas for additional improvements in plant efficiency lie mainly in the catalytic combustor (assuming the fuel cell is state-of-the-art). The catalytic combustor exergetic efficiency was increased in Systems I and II; however, room for further improvement exists. The largest portion of exergy destructions in the combustor are attributable to diffusion processes. One method to reduce this is to

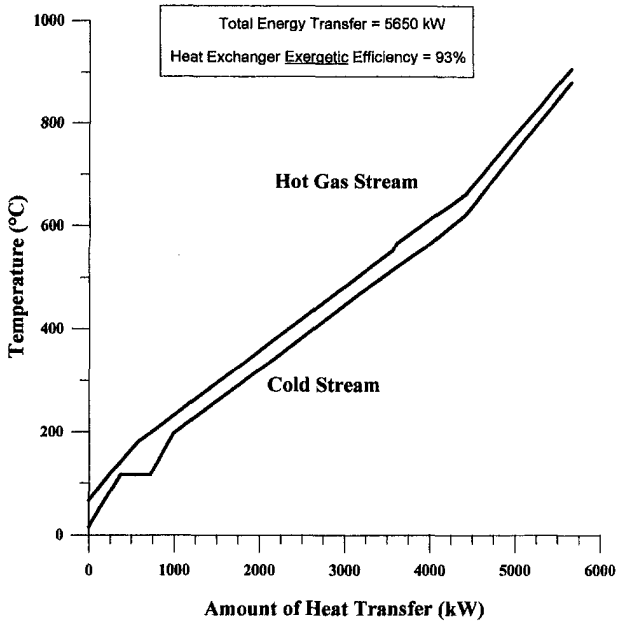

Fig. 11 $T - Q$ diagram, System II: composite curves for new heat exchange network and gas turbine design

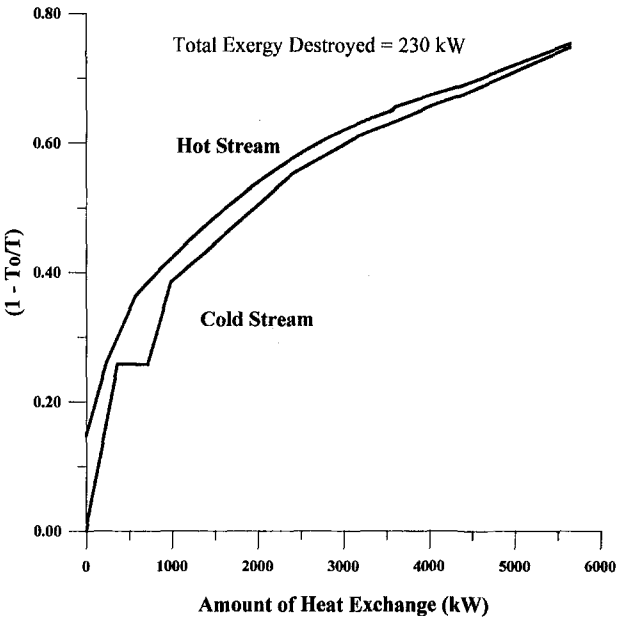

Fig. 12 Composite (1 – *To/T*) versus *Q* diagram, System II: heat exchange network and gas turbine design

split the air stream prior to combustion, for instance, at station 22 in System II, and use only that amount which is necessary for complete combustion at station 7. The remainder of the air flow could be routed to mix with gas flow at station 8 (System II).

Economic factors such as capital, permitting, installation, etc., were not considered in the optimization of this plant. However, it should be noted that, in terms of capital costs, the incremental costs (per kW) for increasing plant power output via the use of well-established technology such as heat exchangers, and steam and gas turbine hardware, would be lower than the expenses for electricity from state-of-the-art MCFC hardware. The capital cost of the *N*th generation MCFC plant was estimated at $1159/kWe in 1990 US$ (EPRI, 1993). The incremental cost evaluation for the addition of steam turbine and associated heat exchanger hardware has been estimated at about $300/kWe (1990 US$) by Lobachyov and Richter (1997). Capital costs for gas turbine hardware, while more expensive than steam turbines, is in the $700–$900/kWe range for distributed power plant sizes. Thus, the incremental costs for adding power output could be reduced if fuel cell systems were integrated with conventional equipment.

References

Dunbar, W. R., and Lior, N., 1994, "Sources of Combustion Irreversibility," *Combustion Science and Technology,* Vol. 103, pp. 41–61.

El-Wakil, M. M., 1984, *Powerplant Technology,* McGraw-Hill, New York, NY.

EPRI TR-102931, 1993, "Applications of Carbonate Fuel Cells to Electric Power Systems," prepared by Fluor Daniel for the Electric Power Research Institute, Final Report.

Kinoshita, K., McLarnon, F. R., and Cairns, E. J., 1988, *Fuel Cells: A Handbook,* DOE/METC-88/6096, prepared for the U.S. Department of Energy, Morgantown, WV.

Linnhoff, B., and Flower, J. R., 1978, "Synthesis of Heat Exchanger Networks," *AIChE Journal,* Vol. 24, No. 4, American Institute of Chemical Engineers, New York, NY.

Linnhoff, B., 1982, *User Guide on Process Integration for the Efficient Use of Energy,* Pergamon Press, New York, NY.

Lobachyov, K. V., and Richter, H. J., 1997, "Addition of Highly Efficient Bottoming Cycles for the *N*th Generation Molten Carbonate Fuel Cell Power Plant," ASME JOURNAL OF ENERGY RESOURCES TECHNOLOGY, Vol. 119, pp. 103–108.

Moran, M. J., and Shapiro, H. N., 1992, *Fundamentals of Engineering Thermodynamics* 2d Edition, Wiley, New York, NY.

Moran, M. J., 1989, *Availability Analysis,* ASME Press, New York, NY.

Rodriguez, L., 1980, "Calculation of Available Energy Quantities," *Thermodynamics: Second Law Analysis,* ACS Symposium Series, Vol. 122, American Chemical Society, Washington, DC.

Williams, K. R., 1966, *An Introduction to Fuel Cells,* Elsevier Publishing Company, New York, NY.

Shinoki, T., Miyazaki, M., Okada, T., Ide, H., and Matsumoto, S., 1992, "Development of Indirect Internal Reforming Molten Carbonate Fuel Cell Stack," *Proceedings, 27th IECEC,* Vol. 3.